東北医科薬科大学

審査学位論文（博士）

氏名（本籍）	リョウ　サイシャ 梁　　彩霞（中国）
学位の種類	博士（薬科学）
学位記番号	博薬科第 25 号
学位授与の日付	令和 4 年 3 月 8 日
学位授与の要件	学位規則第 4 条 1 項該当
学位論文題名	Functional analysis of α1,6-Fucosyltransferase (FUT8) in pancreatic carcinoma cell lines
論文審査委員	主査　　教 授　藤村　務
	副査　　教 授　山口芳樹
	副査　　教 授　顧　建国

Functional analysis of α1,6-Fucosyltransferase (FUT8) in pancreatic carcinoma cell lines

令和 4 年 3 月

東北医科薬科大学大学院薬学研究科

梁彩霞

Contents

1. Introduction

Pancreatic ductal adenocarcinoma (PDAC) accounts for 90% of all pancreatic cancers, which makes it one of the most aggressive forms of malignancy that always has a poor prognosis [1]. PDAC is the fourth-leading cause of cancer-related death in the world, and the 5-year survival rate remains at approximately 5% [2, 3]. The poor survival rate is mainly due to the lack of reliable methods for early detection. In most cases, patients with pancreatic cancer come to the hospital in an advanced inoperable stage. Moreover, pancreatic cancer is highly metastatic and resistant to chemotherapy and radiotherapy [4, 5]. Furthermore, pancreatic cancer is projected to become the second leading cause of cancer-related death within the next decade in the United States based on changing demographics as well as on changes in the incidence and in death rates [6, 7]. Therefore, there is an urgent clinical need to develop novel therapeutic strategies for PDAC.

Abnormal glycosylation changes on the surface of cancer cells have been confirmed as positively related to tumor progression and metastasis, which includes increases in sialylation, fucosylation, and high-branched glycans [8]. Glycoconjugates with altered glycosylation often enter circulation, allowing a clinician to distinguish between patients with and without cancer. Recent research has shown that aberrant glycosylation is common in pancreatic cancer [9, 10]. For example, the sialyltransferase enzymes ST6Gal1 and ST3Gal3 are overexpressed in pancreatic cancer tissue, thereby promoting distant metastasis [11, 12]. Sialyl Lewis A antigen is well known as CA19-9, and it has been used for diagnostic screening and as a tumor marker [13, 14]. Changes in N-glycans are now known to affect the activity of tumor cell surface receptors (EGFR, ErbB2, ErbB3,

and IGF-IR), and thereby affect tumor cell proliferation and survival, which has provided new strategies for tumor treatment [15].

Fucosylation is a common glycosylation type in PDAC, and its increase can be detected in the serum of patients with pancreatic cancer [16-19]. Lectin microarray reveals specific glycosylation alterations in PDAC and normal pancreatic ductal tissues. The reactive abilities with Aleuria aurantia lectin (AAL) and Aspergillus oryzae L-fucose lectin (AOL), which preferentially recognize α1,6-fucose (core fucose) on N-glycans, are obviously higher in cancer tissues than in normal pancreatic ductal tissues [20, 21]. In mammalian cells, core fucosylation of N-glycans is catalyzed by α1,6-fucosyltransferase (FUT8), which catalyzes the transfer of a fucose from GDP-fucose to the innermost GlcNAc residue via α-1,6 linkage [22] (Fig. 1). The intracellular GDP-fucose, an essential substrate of oligosaccharide fucosylation, is generated via two distinct pathways, the *de novo* and salvage pathways [23]. In *de novo* pathway, GDP-mannose is converted to GDP-fucose through enzymatic reactions catalyzed by GDP-mannose 4,6-dehydratase (GMD) and GDP-4-keto-6-deoxymannaose 3,5-epimerase-4-reductase (FX) [24, 25]. In the salvage pathway, GDP-fucose is synthesized by the catalysis of fucose kinase and GDP-fucose pyrophosphorylase [26]. Subsequently, the GDP-fucose is transported into the Golgi complex via the membrane-anchored GDP-L-fucose transporter where GDP-fucose serves as a donor substrate for fucosyltransferases to transfer the fucose to proper N-glycan substrates [27] (Fig. 1).

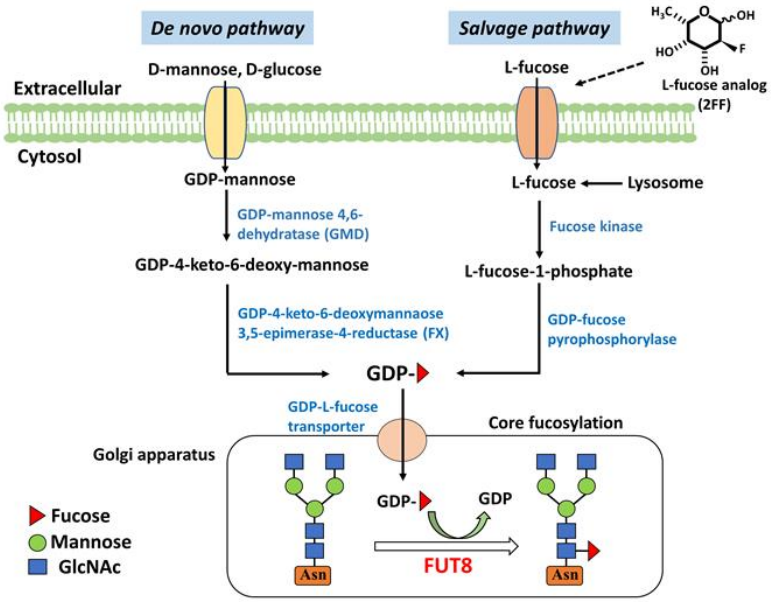

Figure 1. A synthetic pathway for GDP-fucose. GDP-fucose is synthesized through *de novo* and salvage pathways, and is an essential component of core fucosylation. FUT8 is the enzyme responsible for α1,6 core fucosylation, which catalyzes the transfer of a fucose from GDP-L-fucose to the innermost GlcNAc residue via α-1,6 linkage.

In fact, aberrant FUT8 expression and activation has also been observed in other malignant tumors such as liver [28, 29], lung [30], ovarian [31], breast [32], and colorectal [33]. FUT8 is critical for signaling receptors involved in many physiological and pathological processes such as cell growth, adhesion, and tumor metastasis. The core fucosylation of TGF-β receptors facilitates TGF-β ligand binding and EMT in breast tumors [34, 35]. In embryonic fibroblast cells, deficient core fucosylation leads to a blockage of α3β1 integrin-mediated cell migration and cell signaling [36]. Results of our recent study showed that a lack of core fucosylation induced auto-dimerization of Fms-like tyrosine kinase 3 (FLT3) without ligand-stimulation, and several downstream signaling pathways were subsequently activated in acute myeloid leukemia cell lines [37].

In addition, suppression of core fucosylation enhanced the activity of pro-inflammatory cytokines such as IFN-γ and IL-6, resulting in increased sensitivity of microglia and astrocytes in neuroinflammation [38]. These results highlight the multifaceted roles of FUT8 in cancer development and progression. Although several reports have shown that FUT8 is highly expressed in malignant pancreatic cancer [20, 21], the underlying molecular mechanisms of FUT8 in the malignant transformation of PDAC and whether FUT8 could be a potential therapeutic target remains largely unknown.

The present study addressed these questions via in vitro examination of two typical pancreatic cancer cell lines: MIA PaCa-2 and PANC-1 [10, 39]. We used CRISPR/Cas9-mediated gene editing to obtain FUT8 knockout (FUT8-KO) cells from both cell lines. We found that FUT8-KO reduced the cell proliferation and migration of both MIA PaCa-2 and PANC-1 cells and suppressed the characteristics of cancer stem cells (CSCs) such as cancer stem cell biomarker and spheroid formation as well as drug resistance. These results suggest that FUT8 may be a potential therapeutic target for PDAC.

2. Materials and methods

2.1 Antibodies and reagents

The experiments were performed using the following antibodies and reagents: rabbit antibodies against epidermal growth factor receptor (EGFR) (4267S) and peroxidase-conjugated secondary antibody against rabbit (7074S) were purchased from Cell Signaling Technology; mouse antibodies against EGFR (sc-120) were obtained from Santa Cruz Biotechnology; mouse antibodies against α-Tubulin (T6199), peroxidase-conjugated secondary against mouse (AP124P) and fibronectin (F0895) were acquired from MilliporeSigma; mouse antibodies against integrin β1 (P5D2) were obtained from Development Studies Hybridoma Bank; Biotinylated aleuria aurantia lectin (AAL) was purchased from the Seikagaku Corp (Japan); Biotinylated pholiota squarrosa lectin (PhoSL), which specifically recognizes core fucosylated N-glycans, was a gift from Dr. Yuka Kobayashi (J-oil Mills, Tokyo, Japan); goat anti-mouse IgG Alexa Fluor 647 and streptavidin-conjugate Alexa Fluor 647 were obtained from Invitrogen; An ABC kit was acquired from Vector Laboratories; 2-fluoro-L-fucose (2FF), a specific fluorinated analog of fucose, was obtained from Synchem, Inc., IL, USA; Difco TM Agar Noble (214220) was purchased from BD Biosciences; Gemcitabine (G6423) and cycloheximide were purchased from Sigma-Aldrich and Wako, Japan; PrimeScript RT reagent Kit with gDNA Eraser (Perfect Real Time) (RR047A) was purchased from Takara, Japan; Quick Taq HS DyeMix (DTM-101) was purchased from TOYOBO, Japan; and, Dulbecco's modified Eagle's medium (DMEM) and fetal bovine serum (FBS) were obtained from Gibco and Invitrogen, respectively.

2.2 Cell lines and cell culture

Human pancreatic adenocarcinoma cell lines MIA PaCa-2 and PANC-1 were

obtained from the RIKEN cell bank (Japan). These two cell lines were cultured in DMEM supplied with 10% FBS and incubated at 37 °C in a humidified atmosphere containing 5% CO_2. Cells were passaged when the confluence reached approximately 80%.

2.3 RT-PCR for mRNA expression analysis

For each sample, total RNA was extracted from cells using TRIzol Reagent (Invitrogen) according to the manufacturer's instructions. Total RNA (1 μg) was reverse-transcribed using a PrimeScript RT reagent kit (Takara Bio Inc.). The gene expression levels were detected by RT-PCR, and GAPDH was performed as a control. The PCR primer sequences are listed in Table 1. PCR amplification was electrophoresed on 1.5% agarose gel in TBE buffer at 135V for 30 minutes. Finally, the DNA ladder was visualized with ethidium-bromide staining under UV light.

Table 1. Primer sequences for RT-PCR sequences

Target gene	Primer sequences (5′-3′)	
	Forward sequences	Reverse sequences
EpCAM	GCTTTATGATCCTGACTGCG	CAGCCTTCTCATACTTTGCC
CXCR4	GAAGCTGTTGGCTGAAAAGG	TGGAGTGTGACAGCTTGGAG
c-Met	CAATGTGAGATGTCTCCAGC	CCTTGTAGATTGCAGGCAGA
CD133	CAGAGTACAACGCCAAACCA	AAATCACGATGAGGGTCAGC
CD44	TGAGCATCGGATTTGAGAC	CATACTGGGAGGTGTTGGA
CD24	GGCACTGCTCCTACCCACGCAG	GCCACATTGGAATTCCAGACGCC
ALDH1A1	GCACGCC AGACTTACCTGTC	CCTCCTCAGTTGCA GGATTAAAG
GAPDH	CGGAGTCAACGGATTTGGTCGTA	AGCCTTCTCCATGGTGGTGAAGAC

2.4 Generation of CRISPR/Cas9-based FUT8-KO cells and establishment of FUT8 rescued cells.

CRISPR/Cas9-based knockout was performed as described previously with minor modifications [38, 40]. Briefly, guide RNAs targeting the human FUT8 gene were cloned into pSpCas9 (BB)-2A-GFP (PX458) (Addgene, #48138), which was a kind gift from Dr.

Feng Zhang [41]. The plasmids were then electroporated into the MIA PaCa-2 and PANC-1 cells according to the manufacturer's instructions (Amaxa® cell line Nucleofector R kit V). After 2 days of transfection, GFP-positive cells were sorted using FACS Aria II (BD Bioscience). Then negative selections with PhoSL lectin were sorted three times and grown as single clones during 2 to 3 weeks. The FUT8-KO cells were identified via flow cytometric and lectin blot analysis.

To establish a stable rescue cell line, the virus production and infection were performed as described previously [42]. Briefly, the lentivirus vectors (CSIV-TRE-RfA-CMV-KT-FUT8) were transfected into 293T cells with packaging plasmids by calcium phosphate. The target cells were cultured for 48 hours, and the lentivirus supernatants were collected for infection. After infection for 72 hours, the Kusabira Orange-positive cells (CSIV-TRE-RfA-CMV-KT) were sorted using FACSAria II (BD bioscience). Then positive selections with PhoSL lectin were sorted and the stable cell lines were used in subsequent studies.

2.5 Flow cytometry analysis

Cells were detached by brief exposure to 0.25% trypsin containing 1mM EDTA and resuspended at a density of 5×10^6 cells/ml. After washing with ice-cold phosphate buffered saline (PBS), the cells were treated with EGFR (1:500), integrin β1 (1:1000), and biotinylated PhoSL (1:1000) for 1 hour at 4 °C, respectively. Subsequently, cells were incubated with goat anti-mouse IgG Alexa Fluor 647 (1:1000) or streptavidin-conjugate Alexa Fluor 647 (1:1000) for 1 hour at 4 °C in dark. Then, the cells were washed and resuspended in 1ml MACS buffer (PBS containing 0.1% BSA, 1 mM EDTA, and 0.005% NaN_3). Fluorescence data were collected using a FACS Calibur flow cytometer (BD Biosciences, San Jose, CA, USA).

2.6 Western blotting

Western blot analysis was performed according to a procedure established in our previous study [37]. Briefly, the cells were washed twice with cold PBS and then lysed with Tris-buffered saline (TBS) containing 1% Triton X-100, protease inhibitors, and phosphatase inhibitors (Nacalai Tesque, Kyoto, Japan). The resultant mixture was gently blended in a rotor shaker for 1 hour at 4 °C and the supernatant was obtained by centrifugation at 15,000 rpm for 15 minutes at 4 °C. The concentration of lysates was measured via a BCA protein assay kit (Thermo Fisher Scientific, Munich, Germany). The cell lysates were separated on 7.5% SDS–PAGE gel under reducing conditions, and the proteins were transferred to polyvinylidene difluoride (PVDF) membranes (Millipore). After blocking with 5% bovine serum albumin or 5% skim milk, the blots were probed either with each specific antibody or with biotinylated lectin. Immunoreactive bands were performed to analyze the samples by the Immobilon Western Chemiluminescent HRP Substrate (MilliporeSigma).

2.7 Transwell cell migration assay

The effect of FUT8 on cancer cell migration was determined using a 24-well format (8-μm pores; Corning). The bottom of the devices was coated with 10 μg/ml fibronectin overnight at 4 °C and then blocked with 1% BSA in PBS at 37 °C for 1 hour. Cells (1×10^5) in 400 μl of serum-free medium were seeded into the upper chamber. The lower chamber of a 24-well plate contained 500 μl of 10% FBS culture medium. Following incubation times as indicated, cells across pores were fixed with 4% paraformaldehyde and stained with crystal violet solution for 30 minutes. For each chamber, five fields were randomly chosen and cells were counted.

2.8 Wound-healing assay

Briefly, $1x10^6$ human pancreatic cancer cells were seeded into 6-well plates that had been pre-coated with 10 μg/ml fibronectin overnight at 4 °C. A wound was scratched in the confluent cell layer using a 200 μl pipette tip after 24 hours of incubation, and floating cells were gently removed using PBS. Then the cells were continuously cultured in the medium supplemented with 10% FBS for 24 hours. A phase-contrast microscope (Olympus, Tokyo, Japan) was used to record the wound areas at 0 and 24 hours. The migration capability was evaluated by measuring the migration distance.

2.9 Cell growth and colony formation analysis

The cell growth rates were measured using an MTT (#341-01823, Dojindo) assay. MIA PaCa-2 (3×10^3 cells/well) and PANC-1 (5×10^3 cells/well) cells were grown in a 96-well plate at 37 °C in DMEM containing 10% FBS. Every other day until day 3, 10 μl of MTT solution (5 mg/ml in PBS) was added to each well of the plate. After incubating for 4 hours at 37 °C, 100 μl DMSO was added to each well, the absorbance values of each well were measured at 490 nm using a microplate reader (Infinite M1000, TECAN, Japan).

For a colony-formation assay, the different cell lines (1×10^3 cells) were seeded onto 6-well plates in triplicate per cell line, and were then incubated in DMEM containing 10% FBS at 37 °C. The medium was changed twice weekly. After 2 weeks, the cells were fixed with 4% formaldehyde for 20 minutes and then stained with 0.25% crystal violet for 30 minutes. Representative photographs were taken and the colony (containing more than 50 cells) numbers were counted.

2.10 Xenograft assay

The animal experiments in this study were carried out according to guidelines recommended by the Institutional Animal Care and Use Committee and approved by the

Tohoku Medical and Pharmaceutical University Research Ethics Board. Briefly, four-week-old female BALB/c-nu mice were purchased from Charles River Laboratories, Japan. After 1 week of adaptive rearing, wild type and FUT8-KO MIA PaCa-2 cells (3×10^6) in 100 μl PBS were subcutaneously injected into the left and right flanks, respectively (n=6). Tumor sizes were measured by caliper every 5 days and tumor volumes were calculated using the formula $V = 1/2(\text{length} \times \text{width}^2)$. The mice were euthanized at 30 days after injection, and the tumors were photographed and measured.

2.11 Spheroid formation assay

A spheroid culture was conducted by growing cancer cell suspensions in agarose-coated 96-well plates. Briefly, 50 μl of 1.5% (w/v in PBS) agarose was added to each well of the 96-well microplates. Pancreatic cancer cells ($1x10^4$) in 200 μl DMEM medium were then seeded on the pre-coated plates with incubation at 37 °C under 5% CO_2 for 6 days. Half of the supernatant was replaced with fresh medium every 2 days. Spheroid formations were observed and photographed using a phase-contrast microscope (Olympus, Tokyo, Japan). Following culture at indicating times, the spheres were transferred to new plates and the robustness was checked via gentle pipetting.

2.12 Cytotoxicity assay

MTT assays were performed to evaluate cell viability. The same numbers of wild-type and FUT8-KO MIA PaCa-2 and PANC-1 cells ($5x10^3$ cells per well) were seeded onto 96-well plates and exposed to gemcitabine at various concentrations (0, 1, 3, 10, 30 and 100 nM) in the normal culture media. After the MIA PaCa-2 and PANC-1 cells were cultured for 3 and 4 days, respectively, 10 μl of MTT solution (5 mg/ml) was added to each well followed by incubation at 37 °C for 4 hours. The media was then replaced with 100 μl of DMSO, which formed purple formazan crystals when dissolved. Cell viability

was evaluated by reading the plates at an absorbance of 490 nm using a microplate reader (Infinite M1000, TECAN, Japan).

2.13 Statistical analysis

Prism 5.0 software (GraphPad Software, La Jolla, CA, USA) was used to conduct statistical analysis. All data are presented as the mean ± S.E.M. Statistical significance was calculated via a two-tailed unpaired Student's *t* test, and the significance was defined as $P<0.05$ (*$P<0.05$; ** $P < 0.01$; ***$P<0.001$; ns: no significance).

3. Results

3.1 Establishment of FUT8 knockout (FUT8-KO) cells

To understand the mechanisms of FUT8 on the malignant transformation of pancreatic cancer, we established FUT8-KO MIA PaCa-2 and PANC-1 pancreatic cancer cells using the CRISPR/Cas9 system. To verify the FUT8-KO cell lines, the expression levels of core fucosylation on the cell surfaces were examined via flow cytometric analysis using PhoSL (Fig. 2A), and the total expression of fucosylated N-glycans was detected by immunoblotting analysis using AAL (Fig. 2B). Both lectins preferentially recognized the core fucosylated N-glycans. Compared with wild-type (WT) cells, the reactive abilities with AAL or PhoSL were almost abolished in the FUT8-KO cells, which indicated a silencing of the FUT8 gene. What is more, the reactive abilities to AAL were rescued when re-expressing FUT8 in both MIA PaCa-2 and PANC-1 KO cells (Fig. 2B). In addition, we noticed that the FUT8-KO cells, especially for MIA PaCa-2, appeared to be readily aggregated, compared with the WT cells (Fig. 2C). These results suggested that FUT8 has a potential role in regulating the morphological changes of pancreatic cancer cells.

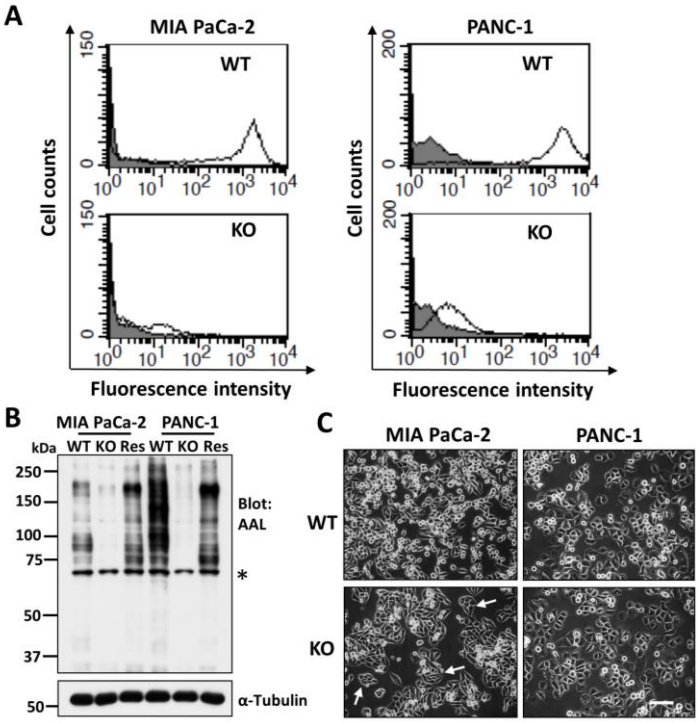

Figure 2. Established FUT8 deficient cells. Establishment of FUT8-KO MIA PaCa-2 and PANC-1 cells. (A) The expression levels of core fucosylation on the cell surface were analyzed by flow cytometry using PhoSL lectin. (B) Equal amounts of cell lysates were detected by AAL lectin blot, and α-Tubulin was used as a loading control. Asterisks indicate the nonspecific bands. (C) Representative cell morphology images were taken using a phase-contrast microscope. Scale bar: 50 μm. WT, wild-type; KO, FUT8 knockout; Res, restoration with FUT8 gene in FUT8-KO cells.

3.2 FUT8-KO suppressed tumor cell migration in vitro

Compared with the WT of MIA PaCa-2 cells, the FUT8-KO significantly suppressed the cell migration, which were demonstrated in the transwell assay (Fig. 3A) and wound-healing assay (Fig. 3C). Consistently, FUT8-KO also significantly decreased cell migration in the transwell assay in PANC-1 cells (Fig. 3B), although this effect was not observed in the wound-healing assay (Fig. 3D). To further confirm that the effects were

indeed caused by the absence of FUT8, we restored FUT8 expression in both KO cells (Res). As expected, the cell migration was greatly improved in the Res cells, by comparison with the KO cells (Fig. 3A, B). Apparently, in both assays, PANC-1 cells moved much faster than MIA PaCa-2 cells, which may suggest that PANC-1 cells have a higher metastatic potential than MIA PaCa-2 cells. These results indicated that the silencing of FUT8 resulted in decreased cell migration in PDAC.

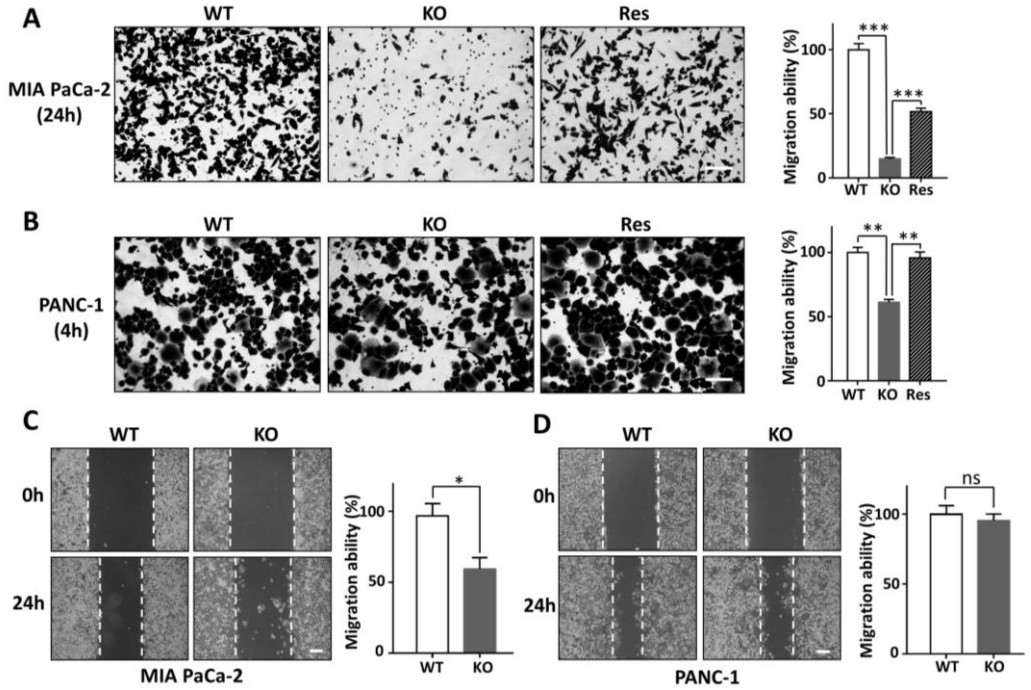

Figure 3. Effects of FUT8-KO on cell migration. Impacts of FUT8-KO on cell migration were measured by transwell and wound-healing assays. The migratory abilities were examined by transwell assay in MIA PaCa-2 for 24 hours (A) and PANC-1 for 4 hours (B). The numbers of migrated cells were counted from three randomly selected areas in each group. The migratory abilities of each WT cells were set as 100. Scale bar: 50 μm. The wound-healing assays were performed in MIA PaCa-2 (C) and PANC-1 (D) cells, and incubated for 24 hours after scratching. The data were obtained from three independent experiments. All values are reported as the mean ± S.E.M (n=3). The

migratory abilities of each of the WT cells were set as 100. Scale bar: 100 μm. *P<0.05; **P<0.01; ***P<0.001; ns: no significance.

3.3 Deficiency of FUT8 inhibited cell proliferation and colony formation

Although an aberrant expression of FUT8 has been identified in different kinds of cancers, its functional contribution to cancers has been inconclusive. The expression of FUT8 was decreased in gastric cancer, and upregulation of FUT8 suppressed the proliferation of gastric cancer cells [43]. By contrast, the FUT8 expression was enhanced in hepatitis B virus-related hepatocellular carcinoma, and the knockdown of FUT8 inhibited the proliferation of tumors [44]. Consistent with that observation, the efficiency of DEN-induced hepatoma was dramatically suppressed in FUT8-KO mice [45]. To investigate the functional roles of FUT8 in PDAC, we conducted MTT and colony formation. The FUT8-KO significantly inhibited cell proliferation in both cells. The restoration with FUT8 gene in the KO cells enhanced cell proliferation (Fig. 4A, B). The colony sizes and numbers were significantly decreased in FUT8-KO cells compared with each of WT cells (Fig. 4C, D). These results supported the notion that FUT8 expression regulates cell proliferation and survival.

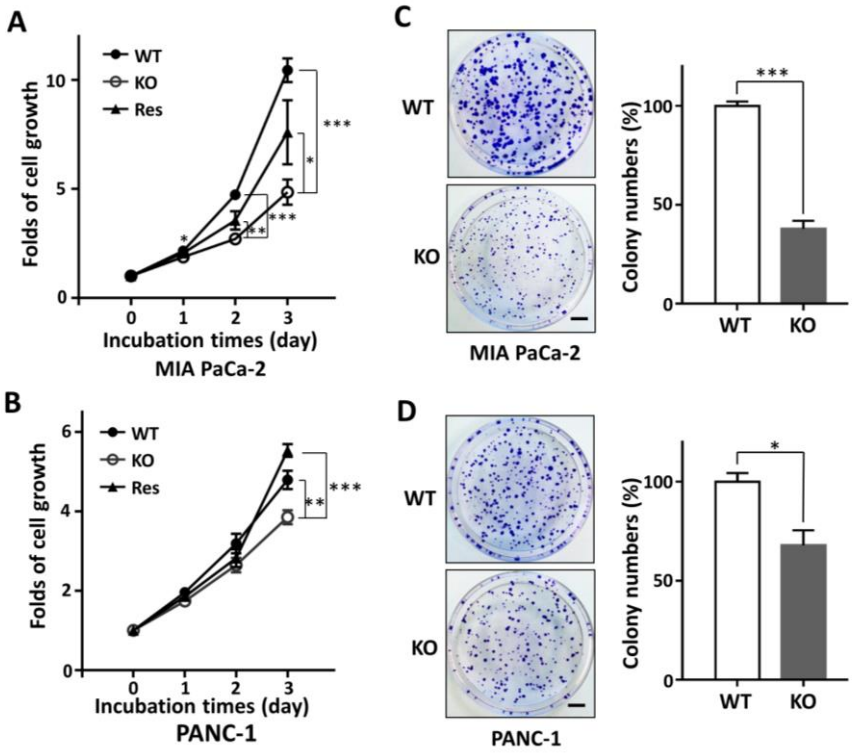

Figure 4. Effects of FUT8-KO on cell proliferation and colony formation. Cell proliferation was measured using MTT as described MATERIALS AND METHODS. The cell numbers were examined at the indicated points in MIA PaCa-2 (A) and PANC-1 (B) cells, and each of the cell numbers seeded into culture wells at 0 day were set as 1. The colony-forming abilities were assayed in MIA PaCa-2 (C) and PANC-1 (D) cells. The data were obtained from three independent experiments. All values are reported as the mean ± S.E.M (n=3). The abilities of each of the WT cells were set as 100. Scale bar: 30 mm. *P<0.05; **P<0.01; ***P<0.001.

3.4 Lack of FUT8 suppressed EGFR expression

Epidermal growth factor receptor (EGFR) is known to play an important role in tumor cell growth and malignancy [46]. EGFR-mediated cellular signaling is crucial for several cancer cell lines such as lung [47] and gastric cancers [48]. In fact, a deficiency

of core fucosylation has down-regulated EGFR-mediated cell signaling and decreased the cell proliferation of non-small cell lung cancer (NSCLC) [49] and fibroblasts [50]. One proposal for an underlying mechanism is that a lack of core fucosylation on EGFR could result in a conformation change that decreases EGF ligand binding, but not EGFR expression. This phenomenon has been observed in HepG2 cells [45, 51]. In the present study, we found that FUT8-KO significantly suppressed the expression of EGFR in MIA PaCa-2 cells. These tendencies were also observed in PANC-1 cells (Fig. 5A, B). The RT-PCR results were shown that there was no significant difference in the mRNA expression levels between WT and KO cells, indicating that deletion of FUT8 does not affect FUT8 expression at transcriptional level (Fig. 5C). To further confirm effects of FUT8-KO on EGFR expression, we checked protein stability using cycloheximide (CHX), an inhibitor of protein synthesis. The expression level of EGFR was significantly decreased in FUT8-KO MIA PaCa-2 cells treated with CHX compared to the untreated cells, but this decrease was not observed in the WT cells (Fig. 5D), suggesting that FUT8 may regulate protein stability. As a control, we also examined the expression of integrin β1 after FUT8 deficiency, which is one of the most abundant cell-surface receptors that is involved in mediating many functional effects such as cell adhesion, migration and intracellular signaling [52]. FUT8-KO did not affect its expression on the cell surface (Fig. 5E). Curiously, the expression levels of β1 in PANC-1 cells were significantly higher than in MIA PaCa-2 cells, which could explain why the migratory abilities of PANC-1 cells were much higher than that in MIA PaCa-2 cells, as shown in Figure 3. Taken together, these results suggest core fucosylation of EGFR regulates both its ligand binding as well as its expression in protein levels.

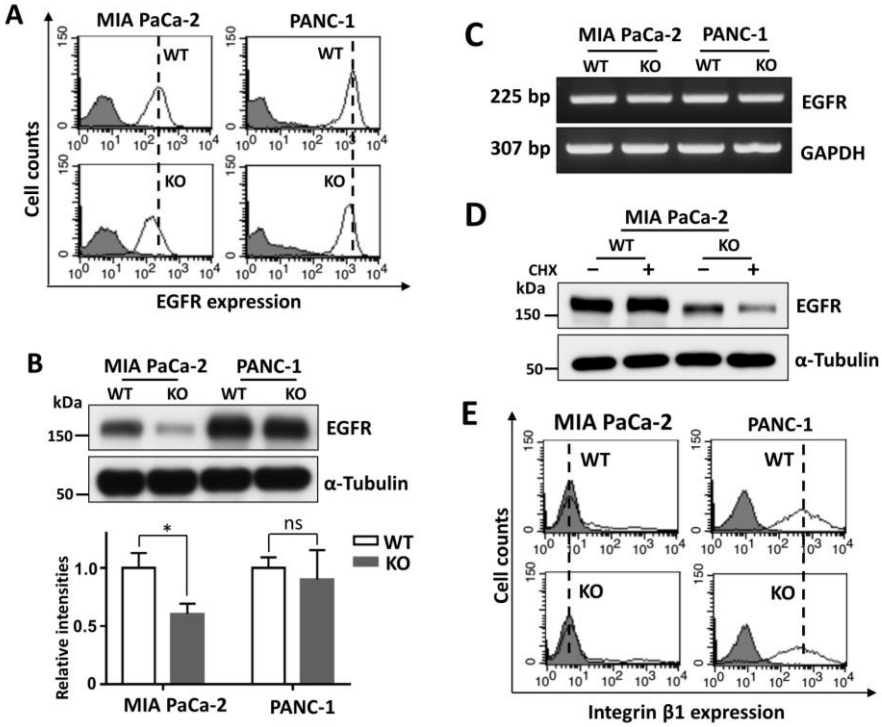

Figure 5. Effects of FUT8 deficiency on EGFR and integrin β1 expression. (A) The expression levels of EGFR on the cell surface were analyzed by flow cytometry assay using an anti-EGFR antibody. (B) The same amounts of cell lysates were probed with EGFR by immunoblotting, and α-Tubulin was used as a loading control. The data were obtained from three independent experiments. All values are reported as the mean ± S.E.M (n=3). *P<0.05; ns: no significance. (C) The mRNA expression levels of EGFR were detected by RT-PCR. GAPDH was used as a control. (D) MIA PaCa-2 cells were treated with cycloheximide (CHX) at 50 μg/mL for 24 hours, and then EGFR levels in cell lysates were monitored by immunoblotting. (E) The expression levels of integrin β1 were analyzed by flow cytometry analysis.

3.5 Inhibitory effect of 2FF on tumorigenesis in vitro

A fluorinated analog of fucose, 2FF, functions as a metabolic fucosylation inhibitor,

which is taken up by cells and converted to GDP-2FF through endogenous salvage pathways [53, 54] (Fig. 1). Therefore, 2FF could be considered a specific inhibitor of fucosylation. In fact, we previously reported that treatment with 2FF could suppress core fucosylation in HepG2 cells [51] as well as in hematopoietic progenitor cells such as Ba/F3 [37]. The inhibitory affects that 2FF exerts on cell migration and growth were verified in FUT8-KO cells. First, we conducted lectin blotting with AAL to insure the efficiency of 2FF as an inhibitor of fucosylation. Those cells were treated with 2FF for 3 days at indicated concentrations, which was followed by a check for reactivity with AAL. In MIA PaCa-2 cells, reactivity with AAL was effectively inhibited by a 2FF concentration as low 30 μM (Fig. 6A, upper panel). By contrast, PANC-1 cells continued to show strong reactivity with AAL with a 2FF concentration of 100 μM, but the inhibitory effect was clearly observed at 500 μM (Fig. 6A, lower panel). These results indicate that 2FF selectively blocks cellular fucosylation in different cells through the salvage pathway for GDP-fucose synthesis. Based on the observations described above, we treated MIA PaCa-2 and PANC-1 cells with 2FF at 100 μM and 500 μM for 3 days, respectively. The migration capabilities of MIA PaCa-2 cells, but not that of PANC-1 cells, seemed to be significantly suppressed by the treatment with 2FF, compared with the control cells (Fig. 6B). An MTT assay, however, showed that 2FF treatment had significantly inhibited cell proliferation in both types of cells (Fig. 6C). Taken together, these results further support the importance of FUT8 in PDAC.

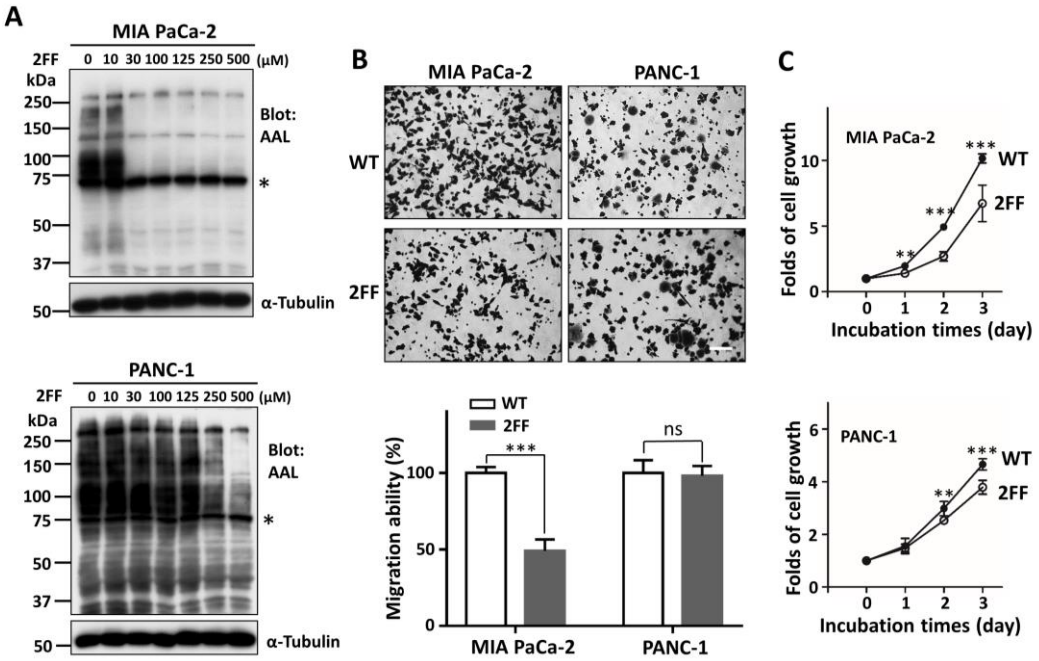

Figure 6. Effects of 2FF on core fucosylation and cell migration as well as proliferation. (A) The cells were cultured with 2FF, an inhibitor of fucosylation, for 3 days at the indicated concentrations. Equal amounts of cell lysates were detected by AAL lectin blot, and α-Tubulin was used as a loading control. Asterisks indicate the nonspecific bands. (B) Cells were pre-treated with or without 2FF for 3 days and seeded ($1x10^5$) into the upper chamber of a transwell. After incubation for 12 and 4 hours for MIA PaCa-2 and PANC-1 cells, respectively, cells across pores were stained with crystal violet and quantitated. The data were obtained from three independent experiments. All values are reported as the mean ± S.E.M (n=3). Scale bar: 50 μm. (C) The cells were cultured with 2FF, and cell proliferation was assessed by MTT assay. The data were obtained from three independent experiments. All values are reported as the mean ± S.E.M (n=3). **P< 0.01; ***P<0.001; ns: no significance.

3.6 Inhibitory effect of FUT8-KO on tumor growth in vivo

To further evaluate the effect of FUT8 on tumor growth, we built xenograft models in nude mice using MIA PaCa-2 cells. Equal amounts of cells ($3x10^6$) were injected subcutaneously into the left and right flanks, respectively. Tumors were isolated on day 30 after injection. We found that FUT8-KO suppressed subcutaneous xenograft growth compared with that in the WT group (Fig. 7A). The tumor volume and weight of the FUT8-KO group were lower than that in the WT group (Fig. 7B, C). The curves for tumor growth in the FUT8-KO group showed a significantly lower rate than those in the WT group (Fig. 7D). These findings suggested that FUT8 deficiency inhibited tumor growth in PDAC in vivo.

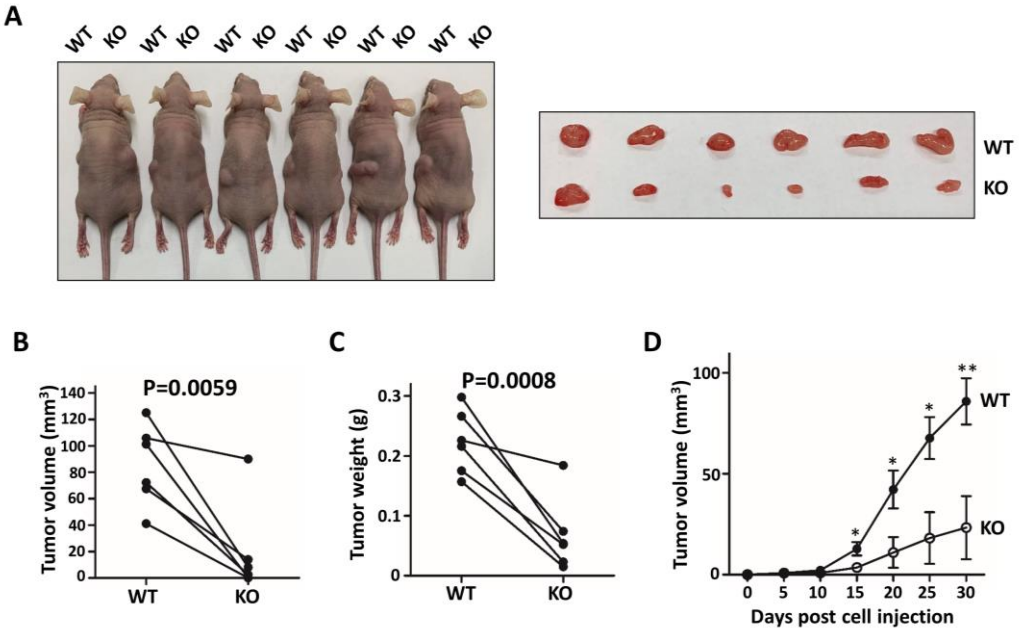

Figure 7. FUT8-KO suppressed tumor growth *in vivo*. Female BALB/c-nu mice were inoculated with MIA PaCa-2 WT and FUT8-KO cells ($3x10^6$) on the left and right flanks, respectively. (A) Images of tumor-bearing nude mice on day 30 after injection were taken after the animals were euthanized (left panel) and each corresponding pair of dissected tumor tissues (right panel). (B) Tumor volume (V) was monitored by measuring the length and width with a vernier caliper and calculated using the formula $V = 1/2(\text{length} \times \text{width}^2)$.

(C) Tumor weight in the two groups was measured using electronic scales. (D) Tumor growth curves for tumor volume were measured every 5 days. *P<0.05; **P<0.01.

3.7 Deficiency of FUT8 downregulated the stemness of pancreatic cancer cells

To understand whether FUT8 expression affects the stem-like characteristics of pancreatic cancer cells, the expression levels of cancer stem cell (CSC)-related biomarkers were examined using RT-PCR. Interestingly, FUT8-KO suppressed the expression levels of biomarkers such as EpCAM, CXCR4, c-Met, and CD133 (Fig. 8A), which suggested that FUT8 may be related to the stemness of pancreatic cancer cells. Since spheroid formation is one of the stem-like characteristics, we compared the abilities to form spheroid bodies among those cells cultured in 96-well plates and pre-coated with a thin layer of 1.5% agarose. As shown in Fig 8B, 8C, the FUT8-KO cells showed a large spheroid body with a loose sphere structure at each of the different incubated times, by comparison with the WT cells in both MIA PaCa-2 and PANC-1 cells. These phenomena were clearly observed after agitation. The spheroid bodies were more easily disrupted in FUT8-KO cells compared with those of the WT cells or those KO cells restored with FUT8 gene.

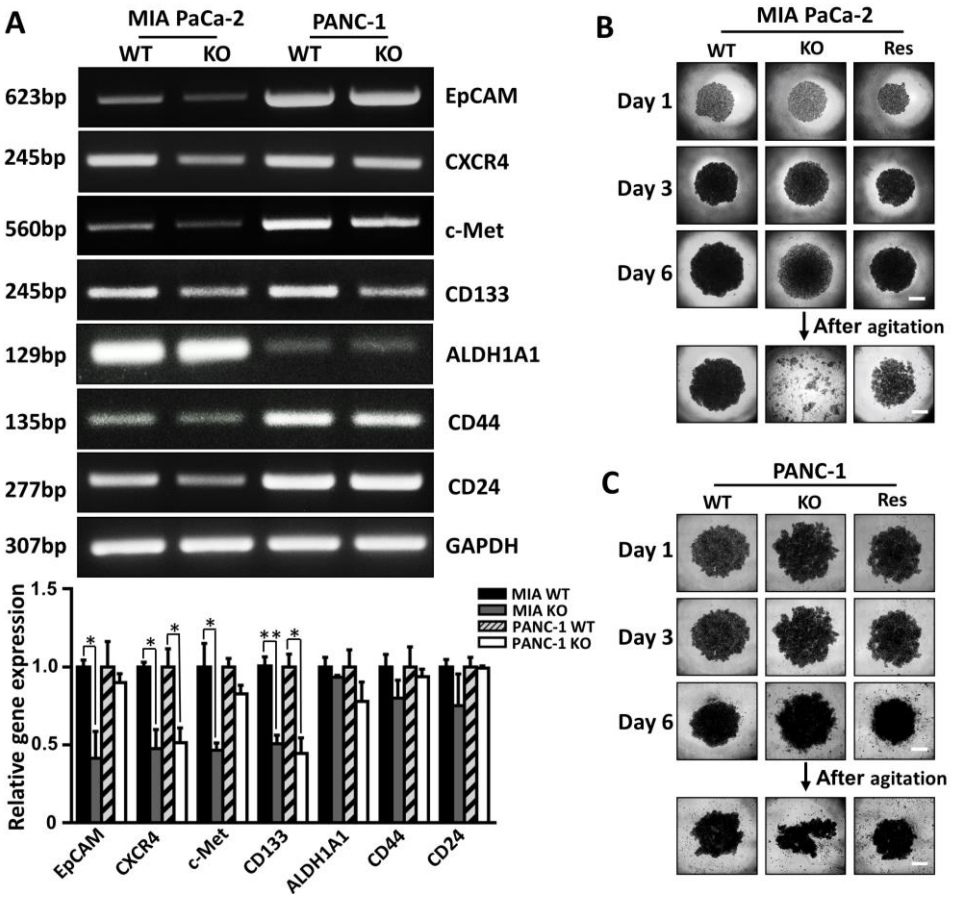

Figure 8. Effects of FUT8-KO on stemness features in MIA PaCa-2 and PANC-1 cells. (A) The mRNA levels of some representative CSC biomarkers were examined by RT-PCR. GAPDH was used as a loading control. The data were obtained from three independent experiments. All values are reported as the mean ± S.E.M (n=3). *P<0.05; **P<0.01. The images of spheroids for MIA PaCa-2 cells (B) and PANC-1 cells (C) were photographed by phase-contrast microscopy at day 1, 3 and 6 of culture. The stability or rigidity of the sphere was checked after agitating using yellow tips and then photographed. Scale bar: 250 μm.

3.8 Deletion of FUT8 increased drug sensitivity

Chemoresistance is also one of the characteristics of CSCs. Gemcitabine is regarded as a standard treatment and has been widely utilized as a first-line therapy for advanced

pancreatic cancer [55, 56]. In order to investigate the effects of FUT8 on drug sensitivities in pancreatic carcinoma, MIA PaCa-2 cells and PANC-1 cells were treated with gemcitabine at indicated concentrations for 3 and 4 days, respectively. As shown in Fig 9A, treatment with low concentrations of gemcitabine significantly suppressed cell viability in FUT8-KO MIA PaCa-2 cells, compared with that in WT cells. A similar trend was also observed in PANC-1 cells (Fig. 9B). Again, these results suggest that the expression of FUT8 may greatly contribute to cancer stemness as well as to cell survival in PDAC.

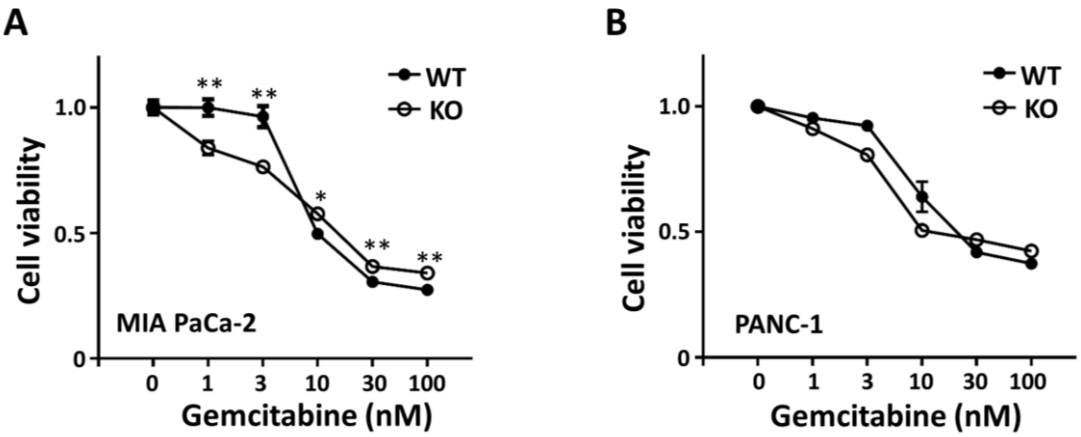

Figure 9. Loss of FUT8 chemosensitized the cells to gemcitabine, an antipancreatic cancer drug. The WT and the FUT8-KO of MIA PaCa-2 cells (A) or PANC-1 cells (B) were cultured in the presence of gemcitabine at indicated concentrations for 3 and 4 days, respectively, and then cell viabilities were examined using MTT assay. The inhibitory ratio for cell viability was normalized to that of each group without gemcitabine as 1. Data are reported as the mean ± S.E.M (n=3). *P<0.05; **P<0.01.

4. Discussion

In the present study, the effects of FUT8 on pancreatic cancer cells were investigated in vivo and in vitro. Using two pancreatic cancer cell models, MIA PaCa-2 and PANC-1, we found that either a deficiency of FUT8 or a blockage of fucosylation using 2FF could suppress cell migration and proliferation, and the subsequent tumor growth, in a subcutaneous xenograft model. Furthermore, FUT8-KO downregulated cancer stemness features, which were evaluated using the expression levels of CSC biomarkers, the capabilities of spheroid formation, and chemoresistance (Fig. 10). These results clearly suggest that regulating core fucosylation may provide a potential therapeutic direction for developing a novel treatment for pancreatic carcinoma.

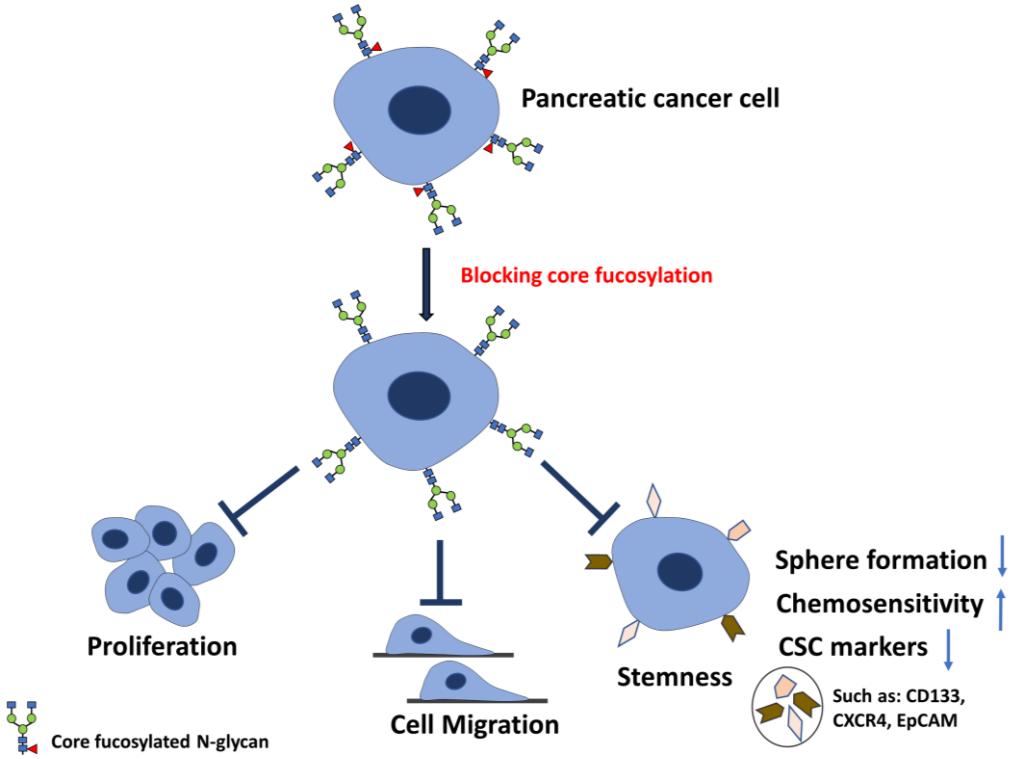

Figure 10. Schematic diagram of core fucosylation in pancreatic cancer. Pancreatic cancer cells are modified with high core fucosylation, inhibition of core fucosylation can inhibit cell proliferation, migration and cancer stemness features

including cancer stem cell biomarkers, spheroid formation and chemoresistance, which could be beneficial to prevent tumor regrowth or recurrence.

CSCs are a very small subpopulation of cells in the tumor population. These cells have the capacity to self-renew and to generate differentiated cancer progenies [57, 58]. The existence of CSCs has been identified in many solid tumors such as lung [59], colorectal [60], breast [61], brain [62], and pancreatic cancers [63]. CSCs not only drive tumor initiation and growth but also mediate tumor metastasis, relapse and chemo/radio-resistance [64-66]. Among these cancers, pancreatic carcinoma tumors have shown relatively higher rates of malignancy and metastasis [67]. Effective therapy for pancreatic cancer remains one of the greatest challenges for public health. Therefore, therapeutic strategies that effectively target CSCs could lend assistance to the treatment of patients with PDAC.

Fucosylated glycan has pivotal roles in tumor development to malignancy and metastasis. Terao et al. reported that cancer stem cell-like pancreatic cancer phenotypes such as gemcitabine-resistant cells, sphere-forming cells, and $CD24^{high}/CD44^{high}$ CSC fractions exhibit much higher levels of fucosylated glycans compared with non-CSC types of cells [68]. In another study, an up-regulation of both fucosyltransferases FUT3 and FUT6 increased SLe^x expression and enhanced the sphere formation and invasion of oral CSCs [69]. Other recent reports have shown an up-regulation of core fucosylation in patients with pancreatic cancer [20, 21]. In the present study, we found that a deficiency of FUT8 significantly decreased the expression levels of CSC biomarkers such as EpCAM, CXCR4, c-Met and CD133 in both MIA PaCa-2 and PANC-1 cells. A similar trend has been observed in other CSC biomarkers such as CD44, CD24 and ALDH1A1 (Fig. 8A). In addition, spheroid formation (the formation of multicellular spheroidal cell

aggregates), which is one of the characteristics of CSCs, has shown that the wild-type cells form structures that are more compact and rigid compared with the corresponding FUT8-KO cells (Fig. 8B, C). Therefore, it would be plausible to speculate that the decreased tumorigenesis of PDAC by FUT8-KO is attributable to its functions in CSCs. In a consistent manner, FUT8-KO greatly increased the chemosensitivity for gemcitabine in MIA PaCa-2 cells (Fig. 9A), since CSCs are known to mediate chemoresistance. Taken together, these data clearly suggest the expression of FUT8 contributes to the stemness features of pancreatic cancer cells. This phenomenon may not be restricted to PDAC, but could also apply to other cancers. In fact, increased core fucosylation has been associated with distal metastasis, tumor recurrence and poorer survival of patients with lung and breast cancers [35, 70], and upregulated FUT8 expression by activation of Wnt/β-catenin signaling pathway could promote EMT and stemness in breast cancer cells [71]. Thus, alterations in core fucosylation could generally have a big impact on the development and progression of other types of cancers.

Notably, the effects of core fucosylation on biological functions may vary among different cell types. For example, FUT8-KO suppressed Smad-2 activation through the TGF-β activation pathway in lung tissue and in fibroblasts [72], but promoted Smad-2 activation via the activin activation pathway in PC12 cells [34]. In the present study, the inhibitory effects on spheroid formation and cell migration by FUT8-KO in PANC-1 cells were smaller than those in MIA PaCa-2 cells (Fig. 3, 8B and C), although a similar tendency was observed. In fact, tumors in different locations may display different clinical parameters and malignant potential. PANC-1 and MIA PaCa-2 cell lines are known to originate from pancreatic head and body/tail cancers, respectively [39]. In the present study, PANC-1 cells exhibited much higher expression levels of metastasis-associated

molecules such as EphA2 and c-Met [73, 74], as well as EpCAM and CD44 compared with the levels expressed by MIA PaCa-2. In addition, PANC-1 cells expressed higher levels of adhesion-associated molecule integrin β1(Fig. 5E). A deficiency of FUT8 in PANC-1 cells did not significantly inhibit cell migration and increase sensitivity to the anticancer drug gemcitabine compared with those in MIA PaCa-2 cells, which led us to speculate that the regulatory functions of FUT8 are dependent on cell type, wherein the expression levels of target glycoproteins for FUT8 are different. Of course, the underlying mechanism for the contribution that FUT8 makes to cancer stemness features will require further study.

Core fucosylation is known to regulate biological functions via the influence of protein expression. We previously reported that FUT8-KO suppressed VEGFR-2 expression and enhanced ceramide-induced cell apoptosis, which contributed to the cause of emphysema-like changes in FUT8-KO mice [75]. In similar manner, blocking core fucosylation by 2FF reduced cell-surface PD-1 expression and the binding of PD-1 to its ligand PDL-1. The effect of 2FF also reversed T cell dysfunction and led to more efficient tumor eradication [76]. Recent study of the molecular mechanism of core fucosylation has shown that its loss enhances the ubiquitination of PD-1 and increases the degradation of PD-1 by proteasomes [77]. In the present study, flow cytometric analysis and anti-EGFR immunoblotting in PDAC showed that FUT8-KO suppresses EGFR protein expression levels (Fig. 5A, B), but not at the transcriptional level, which was confirmed by RT-PCR (Fig. 5C). This result is contradictory to our previous observation that a lack of core fucosylation did not affect EGFR expression on the cell surface, but decreased EGFR-mediated cellular signaling through the down-regulation of ligand binding in embryonic fibroblasts derived from FUT8-KO mice [50]. Considering the association of

EGFR with other receptors such as integrins that may affect endocytosis [78], we speculated that those discrepancies could have been due to cell type, in which expression levels of EGFR-associated proteins are different.

In conclusion, the present study demonstrated some important functions of FUT8 in PDAC progression. FUT8 regulated not only pancreatic tumor proliferation and migration in vitro and tumor growth in vivo, it also affected CSC characteristics that include the expression of CSC biomarkers, spheroid formation, and chemosensitivity. This study is the first to show that FUT8 is involved in the regulation of cancer stemness features, which means that FUT8 is a potential novel target for PDAC treatment.

5. References

1. Bray, F., et al., Global cancer statistics 2018: GLOBOCAN estimates of incidence and mortality worldwide for 36 cancers in 185 countries. CA Cancer J Clin, 2018. **68**(6): p. 394-424.
2. Hidalgo, M., Pancreatic cancer. N Engl J Med, 2010. **362**(17): p. 1605-17.
3. Siegel, R.L., K.D. Miller, and A. Jemal, Cancer statistics, 2020. CA Cancer J Clin, 2020. **70**(1): p. 7-30.
4. Zeng, S., et al., Chemoresistance in Pancreatic Cancer. Int J Mol Sci, 2019. **20**(18).
5. Wei, L., et al., Oncogenic ADAM28 induces gemcitabine resistance and predicts a poor prognosis in pancreatic cancer. World J Gastroenterol, 2019. **25**(37): p. 5590-5603.
6. Rahib, L., et al., Projecting Cancer Incidence and Deaths to 2030: The Unexpected Burden of Thyroid, Liver, and Pancreas Cancers in the United States. Cancer Research, 2014. **74**(11): p. 2913-2921.
7. Kamisawa, T., et al., Pancreatic cancer. Lancet, 2016. **388**(10039): p. 73-85.
8. Pinho, S.S. and C.A. Reis, Glycosylation in cancer: mechanisms and clinical implications. Nat Rev Cancer, 2015. **15**(9): p. 540-55.
9. Munkley, J., The glycosylation landscape of pancreatic cancer. Oncol Lett, 2019. **17**(3): p. 2569-2575.
10. Park, H.M., et al., Mass spectrometry-based N-linked glycomic profiling as a means for tracking pancreatic cancer metastasis. Carbohydr Res, 2015. **413**: p. 5-11.
11. Perez-Garay, M., et al., alpha2,3-Sialyltransferase ST3Gal IV promotes migration and metastasis in pancreatic adenocarcinoma cells and tends to be highly

expressed in pancreatic adenocarcinoma tissues. Int J Biochem Cell Biol, 2013. **45**(8): p. 1748-57.

12. Hsieh, C.C., et al., Elevation of beta-galactoside alpha2,6-sialyltransferase 1 in a fructoseresponsive manner promotes pancreatic cancer metastasis. Oncotarget, 2017. **8**(5): p. 7691-7709.
13. Yue, T., et al., Identification of blood-protein carriers of the CA 19-9 antigen and characterization of prevalence in pancreatic diseases. Proteomics, 2011. **11**(18): p. 3665-74.
14. Luo, G., et al., New observations on the utility of CA19-9 as a biomarker in Lewis negative patients with pancreatic cancer. Pancreatology, 2018. **18**(8): p. 971-976.
15. Contessa, J.N., et al., Inhibition of N-linked glycosylation disrupts receptor tyrosine kinase signaling in tumor cells. Cancer Res, 2008. **68**(10): p. 3803-9.
16. Yue, T., et al., The prevalence and nature of glycan alterations on specific proteins in pancreatic cancer patients revealed using antibody-lectin sandwich arrays. Mol Cell Proteomics, 2009. **8**(7): p. 1697-707.
17. Sawke, N.G. and G.K. Sawke, Serum fucose level in malignant diseases. Indian J Cancer, 2010. **47**(4): p. 452-7.
18. Morishita, K., et al., Haptoglobin phenotype is a critical factor in the use of fucosylated haptoglobin for pancreatic cancer diagnosis. Clin Chim Acta, 2018. **487**: p. 84-89.
19. Gao, H.F., et al., Overexpressed N-fucosylation on the cell surface driven by FUT3, 5, and 6 promotes cell motilities in metastatic pancreatic cancer cell lines. Biochem Biophys Res Commun, 2019. **511**(2): p. 482-489.
20. Tada, K., et al., Fucosyltransferase 8 plays a crucial role in the invasion and

metastasis of pancreatic ductal adenocarcinoma. Surg Today, 2020.

21. Watanabe, K., et al., Fucosylation is associated with the malignant transformation of intraductal papillary mucinous neoplasms: a lectin microarray-based study. Surg Today, 2016. **46**(10): p. 1217-23.

22. Norton, P.A. and A.S. Mehta, Expression of genes that control core fucosylation in hepatocellular carcinoma: Systematic review. World J Gastroenterol, 2019. **25**(23): p. 2947-2960.

23. de Vries, T., et al., Fucosyltransferases: structure/function studies. Glycobiology, 2001. **11**(10): p. 119r-128r.

24. Niittymäki, J., P. Mattila, and R. Renkonen, Differential gene expression of GDP-L-fucose-synthesizing enzymes, GDP-fucose transporter and fucosyltransferase VII. Apmis, 2006. **114**(7-8): p. 539-48.

25. Tonetti, M., et al., Synthesis of GDP-L-fucose by the human FX protein. J Biol Chem, 1996. **271**(44): p. 27274-9.

26. Becker, D.J. and J.B. Lowe, Fucose: biosynthesis and biological function in mammals. Glycobiology, 2003. **13**(7): p. 41r-53r.

27. Puglielli, L. and C.B. Hirschberg, Reconstitution, identification, and purification of the rat liver golgi membrane GDP-fucose transporter. J Biol Chem, 1999. **274**(50): p. 35596-600.

28. Zhang, Y., et al., ESI-LC-MS Method for Haptoglobin Fucosylation Analysis in Hepatocellular Carcinoma and Liver Cirrhosis. Journal of proteome research, 2015. **14**(12): p. 5388-5395.

29. Nie, H., et al., Specific N-glycans of Hepatocellular Carcinoma Cell Surface and the Abnormal Increase of Core-α-1, 6-fucosylated Triantennary Glycan via N-

acetylglucosaminyltransferases-IVa Regulation. Scientific reports, 2015. **5**: p. 16007-16007.

30. Liu, Y.C., et al., Sialylation and fucosylation of epidermal growth factor receptor suppress its dimerization and activation in lung cancer cells. Proc Natl Acad Sci U S A, 2011. **108**(28): p. 11332-7.

31. Takahashi, T., et al., alpha1,6fucosyltransferase is highly and specifically expressed in human ovarian serous adenocarcinomas. Int J Cancer, 2000. **88**(6): p. 914-9.

32. Wi, G.R., et al., A lectin-based approach to detecting carcinogenesis in breast tissue. Oncol Lett, 2016. **11**(6): p. 3889-3895.

33. Osuga, T., et al., Relationship Between Increased Fucosylation and Metastatic Potential in Colorectal Cancer. J Natl Cancer Inst, 2016. **108**(9).

34. Gu, W., et al., α1,6-Fucosylation regulates neurite formation via the activin/phospho-Smad2 pathway in PC12 cells: the implicated dual effects of Fut8 for TGF-β/activin-mediated signaling. Faseb j, 2013. **27**(10): p. 3947-58.

35. Tu, C.F., et al., FUT8 promotes breast cancer cell invasiveness by remodeling TGF-β receptor core fucosylation. Breast Cancer Res, 2017. **19**(1): p. 111.

36. Zhao, Y., et al., Deletion of core fucosylation on alpha3beta1 integrin down-regulates its functions. J Biol Chem, 2006. **281**(50): p. 38343-50.

37. Duan, C., et al., Deficiency of core fucosylation activates cellular signaling dependent on FLT3 expression in a Ba/F3 cell system. Faseb j, 2020. **34**(2): p. 3239-3252.

38. Lu, X., et al., Deficiency of α1,6-fucosyltransferase promotes neuroinflammation by increasing the sensitivity of glial cells to inflammatory mediators. Biochim

Biophys Acta Gen Subj, 2019. **1863**(3): p. 598-608.

39. Ling, Q., et al., The diversity between pancreatic head and body/tail cancers: clinical parameters and in vitro models. Hepatobiliary Pancreat Dis Int, 2013. **12**(5): p. 480-7.

40. Zhang, G., et al., N-acetylglucosaminyltransferase-I as a novel regulator of epithelial-mesenchymal transition. Faseb j, 2019. **33**(2): p. 2823-2835.

41. Ran, F.A., et al., Genome engineering using the CRISPR-Cas9 system. Nat Protoc, 2013. **8**(11): p. 2281-2308.

42. Isaji, T., et al., An oncogenic protein Golgi phosphoprotein 3 up-regulates cell migration via sialylation. J Biol Chem, 2014. **289**(30): p. 20694-705.

43. Zhao, Y.P., et al., Decreased core-fucosylation contributes to malignancy in gastric cancer. PLoS One, 2014. **9**(4): p. e94536.

44. Ji, J., et al., Expression of alpha 1,6-fucosyltransferase 8 in hepatitis B virus-related hepatocellular carcinoma influences tumour progression. Dig Liver Dis, 2013. **45**(5): p. 414-21.

45. Wang, Y., et al., Loss of alpha1,6-fucosyltransferase inhibits chemical-induced hepatocellular carcinoma and tumorigenesis by down-regulating several cell signaling pathways. Faseb j, 2015. **29**(8): p. 3217-27.

46. De Luca, A., et al., The role of the EGFR signaling in tumor microenvironment. J Cell Physiol, 2008. **214**(3): p. 559-67.

47. Leonetti, A., et al., Resistance mechanisms to osimertinib in EGFR-mutated non-small cell lung cancer. Br J Cancer, 2019. **121**(9): p. 725-737.

48. Wang, L., et al., Dual silencing of EGFR and HER2 enhances the sensitivity of gastric cancer cells to gefitinib. Mol Carcinog, 2018. **57**(8): p. 1008-1016.

49. Li, F., et al., α1,6-Fucosyltransferase (FUT8) regulates the cancer-promoting capacity of cancer-associated fibroblasts (CAFs) by modifying EGFR core fucosylation (CF) in non-small cell lung cancer (NSCLC). Am J Cancer Res, 2020. **10**(3): p. 816-837.

50. Wang, X., et al., Core fucosylation regulates epidermal growth factor receptor-mediated intracellular signaling. J Biol Chem, 2006. **281**(5): p. 2572-7.

51. Zhou, Y., et al., Inhibition of fucosylation by 2-fluorofucose suppresses human liver cancer HepG2 cell proliferation and migration as well as tumor formation. Sci Rep, 2017. **7**(1): p. 11563.

52. Barkan, D. and A.F. Chambers, β1-integrin: a potential therapeutic target in the battle against cancer recurrence. Clin Cancer Res, 2011. **17**(23): p. 7219-23.

53. Rillahan, C.D., et al., Global metabolic inhibitors of sialyl- and fucosyltransferases remodel the glycome. Nat Chem Biol, 2012. **8**(7): p. 661-8.

54. Okeley, N.M., et al., Development of orally active inhibitors of protein and cellular fucosylation. Proc Natl Acad Sci U S A, 2013. **110**(14): p. 5404-9.

55. Burris, H.A., 3rd, et al., Improvements in survival and clinical benefit with gemcitabine as first-line therapy for patients with advanced pancreas cancer: a randomized trial. J Clin Oncol, 1997. **15**(6): p. 2403-13.

56. Min, Y.J., et al., Gemcitabine therapy in patients with advanced pancreatic cancer. Korean J Intern Med, 2002. **17**(4): p. 259-62.

57. Kreso, A. and J.E. Dick, Evolution of the cancer stem cell model. Cell Stem Cell, 2014. **14**(3): p. 275-91.

58. Luo, M., et al., Breast cancer stem cells: current advances and clinical implications. Methods Mol Biol, 2015. **1293**: p. 1-49.

59. Maiuthed, A., W. Chantarawong, and P. Chanvorachote, Lung Cancer Stem Cells and Cancer Stem Cell-targeting Natural Compounds. Anticancer Res, 2018. **38**(7): p. 3797-3809.

60. Munro, M.J., et al., Cancer stem cells in colorectal cancer: a review. J Clin Pathol, 2018. **71**(2): p. 110-116.

61. Yang, F., et al., Breast cancer stem cell: the roles and therapeutic implications. Cell Mol Life Sci, 2017. **74**(6): p. 951-966.

62. Lathia, J.D., et al., Cancer stem cells in glioblastoma. Genes Dev, 2015. **29**(12): p. 1203-17.

63. Li, Y., et al., Pancreatic cancer stem cells: emerging target for designing novel therapy. Cancer Lett, 2013. **338**(1): p. 94-100.

64. Dewan, M.Z., et al., Stromal cell-derived factor-1 and CXCR4 receptor interaction in tumor growth and metastasis of breast cancer. Biomed Pharmacother, 2006. **60**(6): p. 273-6.

65. Tanase, C.P., et al., Cancer stem cells: involvement in pancreatic cancer pathogenesis and perspectives on cancer therapeutics. World J Gastroenterol, 2014. **20**(31): p. 10790-801.

66. Visvader, J.E. and G.J. Lindeman, Cancer stem cells in solid tumours: accumulating evidence and unresolved questions. Nat Rev Cancer, 2008. **8**(10): p. 755-68.

67. Amrutkar, M. and I.P. Gladhaug, Pancreatic Cancer Chemoresistance to Gemcitabine. Cancers (Basel), 2017. **9**(11).

68. Terao, N., et al., Fucosylation is a common glycosylation type in pancreatic cancer stem cell-like phenotypes. World J Gastroenterol, 2015. **21**(13): p. 3876-87.

69. Desiderio, V., et al., Increased fucosylation has a pivotal role in invasive and metastatic properties of head and neck cancer stem cells. Oncotarget, 2015. **6**(1): p. 71-84.

70. Honma, R., et al., Expression of fucosyltransferase 8 is associated with an unfavorable clinical outcome in non-small cell lung cancers. Oncology, 2015. **88**(5): p. 298-308.

71. Yang, H.F., et al., Fentanyl Promotes Breast Cancer Cell Stemness and Epithelial-Mesenchymal Transition by Upregulating α1, 6-Fucosylation via Wnt/β-Catenin Signaling Pathway. Front Physiol, 2017. **8**: p. 510.

72. Wang, X., et al., Dysregulation of TGF-beta1 receptor activation leads to abnormal lung development and emphysema-like phenotype in core fucose-deficient mice. Proc Natl Acad Sci U S A, 2005. **102**(44): p. 15791-6.

73. Duxbury, M.S., et al., EphA2: a determinant of malignant cellular behavior and a potential therapeutic target in pancreatic adenocarcinoma. Oncogene, 2004. **23**(7): p. 1448-56.

74. Qian, L.W., et al., Co-cultivation of pancreatic cancer cells with orthotopic tumor-derived fibroblasts: fibroblasts stimulate tumor cell invasion via HGF secretion whereas cancer cells exert a minor regulative effect on fibroblasts HGF production. Cancer Lett, 2003. **190**(1): p. 105-12.

75. Wang, X., et al., Requirement of Fut8 for the expression of vascular endothelial growth factor receptor-2: a new mechanism for the emphysema-like changes observed in Fut8-deficient mice. J Biochem, 2009. **145**(5): p. 643-51.

76. Okada, M., et al., Blockage of Core Fucosylation Reduces Cell-Surface Expression of PD-1 and Promotes Anti-tumor Immune Responses of T Cells. Cell

Rep, 2017. **20**(5): p. 1017-1028.

77. Zhang, N., et al., Loss of core fucosylation enhances the anticancer activity of cytotoxic T lymphocytes by increasing PD-1 degradation. Eur J Immunol, 2020.

78. Hang, Q., et al., Integrin α5 Suppresses the Phosphorylation of Epidermal Growth Factor Receptor and Its Cellular Signaling of Cell Proliferation via N-Glycosylation. J Biol Chem, 2015. **290**(49): p. 29345-60.

6. Abbreviations

AAL: aleuria aurantia lectin

CSC: cancer stem cell

EGFR: epidermal growth factor receptor

FBS: fetal bovine serum

2FF: 2-fluoro-L-fucose

FUT8: α1,6-fucosyltransferase

GAPDH: glyceraldehyde-3-phosphate dehydrogenase

KO: knockout

PBS: phosphate buffered saline

PDAC: pancreatic ductal adenocarcinoma

PhoSL: pholiota squarrosa lectin

WT: wild type

7. Acknowledgments

The three-year study at the Tohoku Medical and Pharmaceutical University is a very important and unforgettable experience for me. Many kind people gave me great support, encouragement and help. Upon the completion of this thesis, I would like to express my sincere appreciation to them.

First and foremost, I owe my sincerely gratitude to President Motoaki Takayanagi for providing the opportunity to study at Tohoku Medical and Pharmaceutical University and provide financial assistance.

Secondly, I would like to show my gratitude to my supervisor, Prof. Jianguo Gu, who has offered me with many important suggestions and valuable guidance both in my study and in my life. The whole process of this thesis from selecting the research topic, analyzing data, and revising manuscripts, Prof. Gu also gave me great instructions and encouragements. Without his patient guidance, the paper cannot be completed.

And also, this thesis can not be accomplished without the consultation and technical supports provided by Dr. Tomohiko Fukuda and Dr. Tomoya Isaji. What is more, I would like to present my thanks to other members of the laboratory. Thanks for the help and encouragement from Ms. Yan Hao, Mr. Chengwei Duan, Ms. Jie Yang, Mr. Feng Qi, and Mr. Wanli Song.

Finally, I would like to show deep gratitude to my family and friends for their kind concern and encouragement. When I was depressed, they listened to my voice and encouraged me to help me regain confidence. Their accompany and support have always been the source of strength for my persistence.